



# Novel aromatic–polyamine conjugates as cholinesterase inhibitors with notable selectivity toward butyrylcholinesterase



Chen Hong<sup>†</sup>, Wen Luo<sup>\*,†</sup>, Dong Yao, Ya-Bin Su, Xin Zhang, Run-Guo Tian, Chao-Jie Wang<sup>\*</sup>

Key Laboratory of Natural Medicine and Immuno-Engineering, Henan University, Kaifeng 475004, People's Republic of China

## ARTICLE INFO

### Article history:

Received 24 February 2014

Revised 29 March 2014

Accepted 29 March 2014

Available online 13 April 2014

### Keywords:

Polyamine conjugates

Alzheimer's disease

Acetylcholinesterase

Butyrylcholinesterase

## ABSTRACT

Three types of aromatic–polyamine conjugates (**6a–6s**) were designed, synthesized and evaluated as potential inhibitors for cholinesterases (ChEs). The results showed that anthraquinone–polyamine conjugates (AQPCs) exhibited the most potent acetylcholinesterase (AChE) inhibitory activity with  $IC_{50}$  values from 1.50 to 11.13  $\mu$ M. Anthracene–polyamine conjugates (APCs) showed a surprising selectivity (from 76- to 3125-fold) and were most potent at inhibiting butyrylcholinesterase (BChE), with  $IC_{50}$  values from 0.016 to 0.657  $\mu$ M. A Lineweaver–Burk plot and molecular modeling studies indicated that the representative compounds, **6l** and **6k**, targeted both the catalytic active site (CAS) and the peripheral anionic site (PAS) of ChEs. Furthermore, APCs did not affect HepG2 cell viability at the concentration of 100  $\mu$ M. Consequently, these polyamine conjugates could be thoroughly and systematically studied for the treatment of AD.

© 2014 Elsevier Ltd. All rights reserved.

## 1. Introduction

Alzheimer's disease (AD) is characterized by dementia, cognitive impairment, and memory loss and is one of the most common diseases in elderly people<sup>1,2</sup> Current treatment of AD focuses on acetylcholinesterase (AChE) inhibitors, such as tacrine, donepezil, rivastigmine and galantamine. However, the potential effectiveness of such inhibitors in clinical use is often complicated by their associated side effects. For example, clinical studies have shown that the AChE inhibitor tacrine causes hepatotoxicity.<sup>3</sup> Since AD is a multi-pathogenic illness, a current drug-discovery strategy is to develop novel anti-Alzheimer agents with multiple potencies such as inhibition of both AChE and butyrylcholinesterase (BChE).<sup>4</sup>

Two major ChEs, AChE and BChE, are involved in the hydrolysis and regulation of acetylcholine in vertebrates. Various cholinergic drugs, primarily inhibitors of AChE also function as BChE inhibitors.<sup>5</sup> The use of agents with enhanced selectivity for BChE including cymserine and MF-8622 indicated potential therapeutic benefit of inhibiting BChE in AD and related dementias. BChE specific inhibition is unlikely to be associated with adverse events and may show efficacy without remarkable side effects.<sup>6</sup> Therefore BChE may be considered as an important target for novel drug development to treat AD. In the future, the development of specific BChE

inhibitors and the continued use of cholinesterase inhibitors may lead to improved clinical outcomes.<sup>7</sup>

Polyamines such as putrescine, spermidine and spermine (Fig. 1) are aliphatic molecules with amine groups distributed along their structure and are the most common natural products. These compounds have always been regarded by medicinal chemists as a universal template<sup>8</sup> and many research groups have chosen to focus their investigations on the polyamine metabolic cycle or the design of polyamine modified drugs.<sup>9–12</sup> Our group has chosen to focus on the development of polyamine conjugates as potential drugs for the treatment of cancer and AD for many years.<sup>13–16</sup> Our research has found that quinoline–polyamine conjugates exhibit potent ChEs inhibitory activity and that polyamines occupy the gorge of AChE.<sup>17</sup> Therefore, to further explore the anti-Alzheimer potential of the polyamine conjugates, we designed and synthesized three types of aromatic–polyamine conjugates and screened them for their ability to inhibit ChEs.

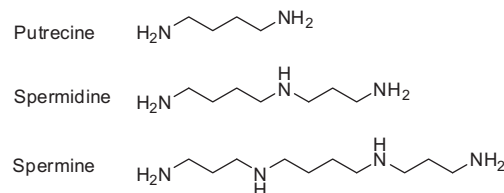


Figure 1. Chemical structures of putrescine, spermidine and spermine.

\* Corresponding authors. Tel./fax: +86 0371 22864665.

E-mail addresses: [luowen83@henu.edu.cn](mailto:luowen83@henu.edu.cn) (W. Luo), [wcsjxq@henu.edu.cn](mailto:wcsjxq@henu.edu.cn) (C.-J. Wang).

<sup>†</sup> The first two authors contributed equally to this work.

## 2. Results and discussion

### 2.1. Chemistry

It is report that many aromatic polycyclic such anthrarobin and anthraquinone have shown diverse activity depending on the functional groups attached<sup>18,19</sup> In this paper we chose three kinds of aromatic polycyclic building blocks (naphthalene, anthracene and anthraquinone) that are coupled to diverse polyamine motifs (Fig. 2) to evaluate their inhibition ability to ChEs. The synthesis of compound **2** was shown in [Supplementary data](#), polyamine skeletons **4e–4j** were synthesized in our lab<sup>16</sup> and the target compounds were synthesized according to [Scheme 1](#). Intermediates **1a**, **2a**, **3a** were obtained by the condensation of chloroacetyl chloride with **1**, **2** and **3** as the starting material. The reaction of **1a–3a** with amines **4a–4j** gave the intermediates **5a–5s**, and their Boc groups in the polyamine skeleton were subsequently removed with 4 M HCl at room temperature to provide hydrochloride salt target compounds. The structures of the target compounds were confirmed by <sup>1</sup>H NMR, ESI-MS and elemental analysis.

### 2.2. In vitro inhibition studies on AChE and BChE

To determine the potential effectiveness of the target compounds **6a–6s** for the treatment of AD, their ChEs inhibitory activity was determined by the method described by Ellman et al.,<sup>20</sup> using tacrine as a reference compound. The IC<sub>50</sub> values for ChEs inhibition and the selectivity index (SI) are summarized as shown in [Table 1](#). Due to their poor solubility, compounds **6f** and **6g** were not measured. Generally, most of the synthetic compounds tested (**6b–6d**, **6h–6o**) showed inhibitory selectivity for BChE over AChE. Anthraquinone–polyamine conjugates (AQPCs) (**6p–6s**) inhibited AChE better than naphthalene–polyamine conjugates (NPCs) and anthracene–polyamine conjugates (APCs), while APCs **6h–6o** exhibited the most potent inhibition of BChE.

Compounds **6l**, **6q** and **6r** were the most potent inhibitors of AChE and had an IC<sub>50</sub> value of 2.74, 1.50 and 2.63 μM, respectively, while compounds **6k** and **6i**, the most potent inhibitors of BChE, had IC<sub>50</sub> value of 0.016 and 0.023 μM, respectively, which were much lower than that of tacrine (IC<sub>50</sub> = 0.037 μM). Moreover, a

compound's ability to inhibit enzyme activity was directly proportional to the chain length of its polyamine moiety such that four (**6k**) and six (**6l**) methylene groups was the optimal chain length between two nitrogen atoms associated with the most potent inhibition of BChE. When the distance between these two nitrogen atoms is too long or too short, the compound is unable to optimally inhibit BChE.

All of the synthetic anthracene conjugates showed high selectivity for BChE over AChE and the ratio of BChE/AChE selectivity ranged from 76- to 3125-fold. The selectivity ratios of compounds were dependent on their inhibitory potential against BChE. The compounds showed higher inhibitory potential against BChE that would possess higher BChE/AChE selectivity ratios. Compounds **6k** showed the highest inhibitory activity (IC<sub>50</sub> = 16 nM) and also had the highest selectivity ratio (3125-fold). This result indicated that the anthracene conjugates could favor binding to BChE.

### 2.3. Kinetic characterization of ChEs inhibition

Graphical analysis of steady state inhibition of the most potent compounds for AChE and BChE, APCs **6l** and **6k**, were investigated to determine the kinetics of ChEs inhibition as shown in [Figure 3](#).<sup>21</sup> The Lineweaver–Burk plots showed both increasing slopes and increasing intercepts for higher inhibitor concentration. The pattern indicated a mixed-type inhibition, hence this kinetic study suggested that compound **6l** bound to both catalytic active site (CAS) and the peripheral anionic site (PAS) of AChE. A similar interaction was found between **6k** and BChE.

### 2.4. Molecular modeling study

To investigate the interaction mode of compound **6l** with TcAChE (PDB code: 1ACJ), molecular modeling was carried out by AUTODOCK 4.0 package with PyMOL program as shown in [Figure 4](#).<sup>22,23</sup> The docking result demonstrated that compound **6l** exhibited multiple binding modes with AChE. In the **6l**–TcAChE complex, compound **6l** occupied the entire enzymatic CAS, mid-gorge and PAS. The anthracene moiety was bound to CAS, displaying a classic π–π stacking interaction between Trp84 and Phe330. At the PAS, the end protonated nitrogen atom of the polyamine

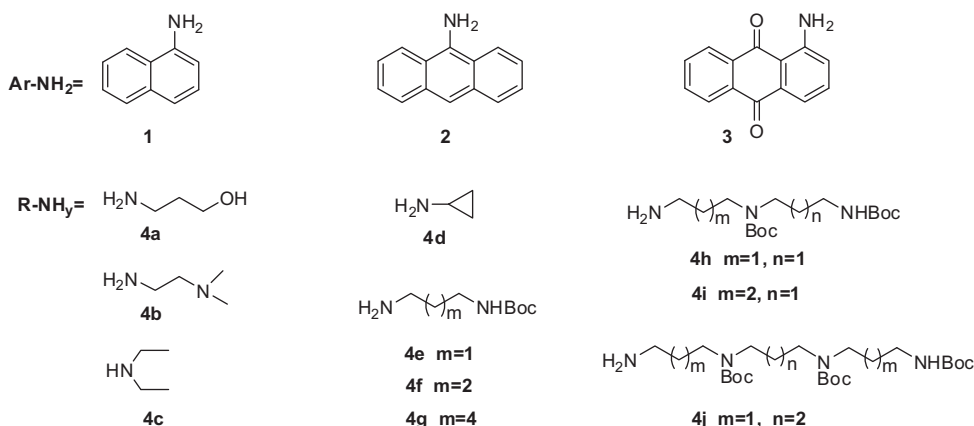
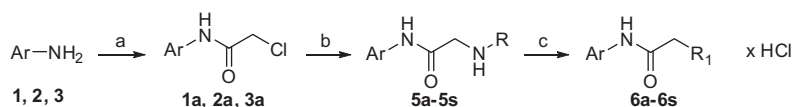
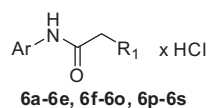


Figure 2. Building blocks of the designed library.



Scheme 1. Reagents and conditions: ClCOCH<sub>2</sub>Cl, THF, Et<sub>3</sub>N, rt, 6 h for **1a** and **2a**; ClCOCH<sub>2</sub>Cl, DMF, pyridine, rt, 24 h for **3a**; (b) 1.0 equiv of R–NH<sub>2</sub>, EtOH, Et<sub>3</sub>N, reflux, 6 h for **5a–5o**; 1.0 equiv of R–NH<sub>2</sub>, CH<sub>3</sub>CN, K<sub>2</sub>CO<sub>3</sub>, KI, rt, 24 h for **5p–5s**; (c) 4 M HCl, EtOH, rt, overnight.

**Table 1**  
Inhibition of ChEs activity and selectivity index of the synthesized compounds



Compds	Ar	R <sub>1</sub>	x	IC <sub>50</sub> <sup>a</sup> for AChE (μM)	IC <sub>50</sub> <sup>b</sup> for BChE (μM)	Selectivity index <sup>c</sup>
<b>6a</b>			1	>50	>50	–
<b>6b</b>			2	>50	4.39 ± 0.17	>11.4
<b>6c</b>			2	>50	10.28 ± 0.04	>4.9
<b>6d</b>			3	>50	47.55 ± 2.02	>1.1
<b>6e</b>			4	>50	>50	–
<b>6f<sup>d</sup></b>			1	–	–	–
<b>6g<sup>d</sup></b>			1	–	–	–
<b>6h</b>			1	>50	0.502 ± 0.041	>99.6
<b>6i</b>			2	>50	0.161 ± 0.004	>310.6
<b>6j</b>			2	>50	0.280 ± 0.007	>178.6
<b>6k</b>			2	>50	0.016 ± 0.001	>3125
<b>6l</b>			2	2.74 ± 0.12	0.023 ± 0.002	119.1
<b>6m</b>			3	>50	0.305 ± 0.007	>163.9
<b>6n</b>			3	25.11 ± 2.24	0.164 ± 0.002	153.1
<b>6o</b>			4	>50	0.657 ± 0.015	>76.1
<b>6p</b>			1	11.13 ± 0.36	>50	<0.20
<b>6q</b>			2	1.50 ± 0.24	>50	<0.03
<b>6r</b>			3	2.63 ± 0.15	32.96 ± 0.71	<0.08
<b>6s</b>			4	7.22 ± 0.24	>50	<0.14
Tacrine		–	–	0.215 ± 0.001	0.037 ± 0.004	5.8

<sup>a</sup> AChE from *electric eel*; IC<sub>50</sub>, 50% inhibitory concentration (means ± SEM of three experiments).

<sup>b</sup> BChE from *equine serum*; IC<sub>50</sub>, 50% inhibitory concentration (means ± SEM of three experiments).

<sup>c</sup> Selectivity index = IC<sub>50</sub> (AChE)/IC<sub>50</sub> (BChE).

<sup>d</sup> Due to the poor solubility, compounds **6f** and **6g** were not measured.

establishes a cation–π interaction with Trp279. The result showed that compound **6l** was able to bind both CAS and PAS of AChE which was in agreement with the result of kinetic study. Because the crystal structure of BChE from equine serum has not been reported, so we did not perform the docking study for compound **6k** with BChE.

### 2.5. Methyl thiazolyl tetrazolium (MTT) assay of HepG2 cell viability

To determine the potential cytotoxic effect of our synthesized compounds, the human hepatoma cell line HepG2 was treated

with our target compounds. As shown in Table 2, the results indicated that NPCs (**6a–6e**) and APCs (**6h–6o**), showed no obvious effect on cell viability at concentrations of 100 μM, compared with tacrine, they had lower toxicity on cell viability. In the case of AQPCs (**6p–6s**), they showed more toxicity than NPCs and APCs with IC<sub>50</sub> value from 11.52 to 24.25 μM, but were less toxic than mitoxantrone.

### 3. Conclusion

In summary, three types of novel aromatic–polyamine conjugates **6a–6s** were synthesized and subjected to biological evaluation.

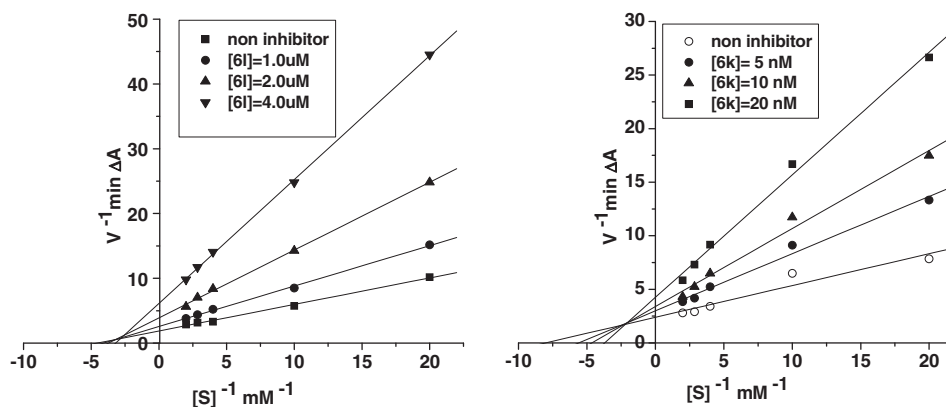


Figure 3. Lineweaver–Burk plot for compound **6l** (left) and **6k** (right) with AChE and BChE, respectively.

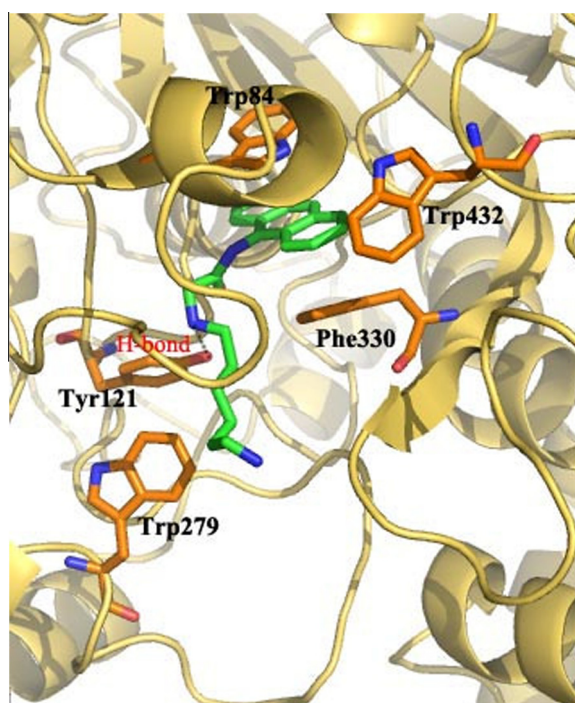


Figure 4. Docking model for compound **6l** with AChE.

The results have shown that AQPCs were moderately potent AChE inhibitors with  $IC_{50}$  values at the micromolar range, APCs were selective and the most potent inhibitors of BChE, the range of BChE/AChE selectivity was from 76- to 3125-fold, and conjugates **6k** and **6l** had an  $IC_{50}$  value of 0.016 and 0.023  $\mu$ M, respectively, which were much lower than that of tacrine. A Lineweaver–Burk plot and molecular modeling study showed that **6k** and **6l** targeted both the CAS and PAS of ChEs. In addition, the APCs did not show obvious toxicity on HepG2 cell viability at 100  $\mu$ M in vitro. These novel polyamine conjugates, especially APCs should be further evaluated as potent, low hepatotoxic ChEs inhibitors for the treatment of AD.

## 4. Experimental section

### 4.1. Chemistry

$^1H$  NMR spectra were recorded with a Bruker AV-400 spectrometer at 400 MHz. MS spectra were recorded on a Shimadzu LCMS-2010A instrument with an ESI mass selective detector. Elemental

Table 2

MTT assay of HepG2 cell viability

Compds	$IC_{50}^a$ ( $\mu$ mol/L)
<b>6a</b>	>100
<b>6b</b>	>100
<b>6c</b>	>100
<b>6d</b>	>100
<b>6e</b>	>100
<b>6f<sup>b</sup></b>	–
<b>6g<sup>b</sup></b>	–
<b>6h</b>	>100
<b>6i</b>	>100
<b>6j</b>	>100
<b>6k</b>	>100
<b>6l</b>	>100
<b>6m</b>	>100
<b>6n</b>	>100
<b>6o</b>	>100
<b>6p</b>	22.96 $\pm$ 3.59
<b>6q</b>	24.25 $\pm$ 2.04
<b>6r</b>	15.64 $\pm$ 1.41
<b>6s</b>	11.52 $\pm$ 0.82
Tacrine	98.73 $\pm$ 3.42
Mitoxantrone	11.05 $\pm$ 1.60

<sup>a</sup>  $IC_{50}$ , 50% inhibitory concentration for HepG2 of target compounds, (mean  $\pm$  SEM of three experiments).

<sup>b</sup> Due to the poor solubility, compounds **6f** and **6g** were not measured.

analyses were performed on a Gmbe VarioEL Elemental Instrument. Flash column chromatography was performed with silica gel (200–300 mesh) purchased from Qingdao Haiyang Chemical Co. Ltd.

### 4.2. General procedures for the preparation of intermediate **1a** and **2a**

A mixture of compound **1** (4.30 g, 30 mmol), triethylamine (8.35 mL, 60 mmol) and THF (50 mL) were stirred at ice bath until completely dissolved, and then chloroacetyl chloride (6 mL, 75 mmol) was added dropwise. The suspension was stirred for 6 h (monitored by TLC). And then the solvent was removed in vacuum, the residue was poured into water and filtered, and the filter cake was washed by water, dried to obtain brown solid, which was purified by flash chromatography to give white solid **1a**. Yield 80%,  $^1H$  NMR (400 MHz, DMSO- $d_6$ )  $\delta_H$ : 10.29 (br s, 1H), 8.05 (d,  $J$  = 7.5 Hz, 1H), 7.96 (d,  $J$  = 9.2 Hz, 1H), 7.81 (d,  $J$  = 8.1 Hz, 1H), 7.68 (d,  $J$  = 7.2 Hz, 1H), 7.55–7.60 (m, 2H), 7.52 (t,  $J$  = 7.8 Hz, 1H), 4.45 (s, 2H). ESI-MS  $m/z$ : 220.7 (M+H)<sup>+</sup>.

9-Aminoanthracene **2** was treated with chloroacetyl chloride according to general procedure to give the intermediate **2a** as yellow solid. Yield 89%,  $^1H$  NMR (400 MHz, DMSO- $d_6$ )  $\delta_H$ : 10.60 (brs,

1H), 8.63 (s, 1H), 8.09–8.15 (m, 4H), 7.53–7.60 (m, 4H), 4.60 (s, 2H). ESI-MS *m/z*: 270.1 (M+H)<sup>+</sup>.

#### 4.3. Procedures for the preparation of intermediate 3a

A mixture of 1-aminoanthraquinone **3** (1.8 g, 8 mmol), pyridine (1 mL) and DMF (70 mL) were stirred at ice bath until completely dissolved, then chloroacetyl chloride (2.8 g, 24 mmol) was added dropwise, the suspension was stirred for 24 h at room temperature. After the reaction finished (monitored by TLC), the reaction was poured into ice water and filtered, the filter cake was washed by ether and recrystallized from EtOH to give pale yellow solid **3a**. Yield 66%, <sup>1</sup>H NMR (400 MHz, DMSO-*d*<sub>6</sub>) δ<sub>H</sub>: 12.72 (br s, 1H), 8.98 (d, *J* = 8.3 Hz, 1H), 8.25 (d, *J* = 8.5 Hz, 1H), 8.18 (d, *J* = 8.4 Hz, 1H), 8.01 (d, *J* = 7.6 Hz, 1H), 7.92–7.96 (m, 3 H), 4.59 (s, 2H). ESI-MS *m/z*: 300.7 (M+H)<sup>+</sup>.

#### 4.4. Procedures for the preparation of material 4h, 4i and 4j

The Boc protected polyamines **4h**, **4i** and **4j** were prepared in our previous work.<sup>16</sup>

#### 4.5. General procedures for the preparation of intermediates 5a–5o

A mixture of **1a** or **2a** (3 mmol), Et<sub>3</sub>N (6 mL), **4a–4j** (4.5 mmol), and 20 mL EtOH were stirred for 6 h under reflux (monitored by TLC). After cooling to the room temperature, the solvent was removed, the residue was diluted with CH<sub>2</sub>Cl<sub>2</sub> (35 mL) and washed with 10% NaCO<sub>3</sub> (30 mL × 3). The organic layer was dried over Na<sub>2</sub>SO<sub>4</sub>, filtered, concentrated in vacuo, and purified by flash column chromatography with chloroform/methanol elution.

#### 4.6. General procedures for the preparation of intermediates 6a–6o

The respective *N*-Boc protected intermediates **5a–5o** were dissolved in EtOH (10 mL) and stirred at 0 °C for 10 min. Then 4 M HCl was added dropwise at 0 °C. The reaction mixture was stirred at room temperature overnight and a white precipitate was generated. The precipitate was concentrated and washed several times with absolute ethanol and ether, and dried under vacuum to give the pure target compounds **6a–6o**.

#### 4.7. 2-(3-Hydroxypropylamino)-*N*-(naphthalen-1-yl)acetamide hydrochloride (6a)

White solid, yield 67.1%, <sup>1</sup>H NMR (400 MHz, D<sub>2</sub>O) δ<sub>H</sub>: 8.08–8.10 (m, 1H), 8.02 (t, *J* = 7.2 Hz, 2H), 7.63–7.73 (m, 4H), 4.38 (s, 2H), 3.83 (t, *J* = 11.9 Hz, 2H), 3.40 (t, *J* = 14.8 Hz, 2H), 2.06–2.12 (m, 2H). ESI-MS *m/z*: 259.1 (M+H–HCl)<sup>+</sup>. Anal. calcd for C<sub>15</sub>H<sub>19</sub>ClN<sub>2</sub>O<sub>2</sub>: C, 61.12; H, 6.50; N, 9.50; found: C, 61.11; H, 6.56; N, 9.42.

#### 4.8. 2-(2-(Dimethylamino)ethylamino)-*N*-(naphthalen-1-yl)acetamide hydrochloride (6b)

White solid, yield 68.4%, <sup>1</sup>H NMR (400 MHz, D<sub>2</sub>O) δ<sub>H</sub>: 8.09–8.12 (m, 1H), 8.04 (t, *J* = 6.7 Hz, 2H), 7.64–7.72 (m, 4H), 4.48 (s, 2H), 3.71–3.79 (m, 4H), 3.09 (s, 6H). ESI-MS *m/z*: 272.1 (M+H–2.3HCl)<sup>+</sup>. Anal. calcd for C<sub>16</sub>H<sub>23</sub>Cl<sub>2</sub>N<sub>3</sub>O·0.3 HCl·0.4 H<sub>2</sub>O: C, 53.02; H, 6.70; N, 11.59; found: C, 52.93; H, 6.99; N, 11.64.

#### 4.9. 2-(4-Aminobutylamino)-*N*-(naphthalen-1-yl)acetamide hydrochloride (6c)

White solid, yield 72.3%, <sup>1</sup>H NMR (400 MHz, D<sub>2</sub>O) δ<sub>H</sub>: 8.08–8.10 (m, 1H), 8.02 (t, *J* = 7.8 Hz, 2H), 7.61–7.72 (m, 4H), 4.38 (s,

2H), 3.33 (t, *J* = 7.2 Hz, 2H), 3.13 (t, *J* = 7.6 Hz, 2H), 1.82–1.98 (m, 4H). ESI-MS *m/z*: 272.2 (M+H–2HCl)<sup>+</sup>. Anal. calcd for C<sub>16</sub>H<sub>23</sub>Cl<sub>2</sub>N<sub>3</sub>O·0.9 H<sub>2</sub>O: C, 53.31; H, 6.93; N, 11.66; found: C, 53.45; H, 6.98; N, 11.68.

#### 4.10. 2-(4-(3-Aminopropylamino)butylamino)-*N*-(naphthalen-1-yl)acetamide hydrochloride (6d)

White solid, yield 71.8%, <sup>1</sup>H NMR (400 MHz, D<sub>2</sub>O) δ<sub>H</sub>: 8.07–8.10 (m, 1H), 8.02 (t, *J* = 6.8 Hz, 2H), 7.62–7.72 (m, 4H), 4.38 (s, 2H), 3.33 (t, *J* = 6.8 Hz, 2H), 3.15–3.25 (m, 6H), 2.12–2.20 (m, 2H), 1.89–1.95 (m, 4H). ESI-MS *m/z*: 329.3 (M+H–3HCl)<sup>+</sup>. Anal. calcd for C<sub>19</sub>H<sub>31</sub>Cl<sub>3</sub>N<sub>4</sub>O·0.6 H<sub>2</sub>O: C, 50.87; H, 7.23; N, 12.49; found: C, 50.99; H, 7.40; N, 12.44.

#### 4.11. 2-(3-(4-(3-Aminopropylamino)butylamino)propylamino)-*N*-(naphthalen-1-yl)acetamide hydrochloride (6e)

White solid, yield 75.2%, <sup>1</sup>H NMR (400 MHz, D<sub>2</sub>O) δ<sub>H</sub>: 8.07–8.10 (m, 1H), 8.02 (t, *J* = 6.8 Hz, 2H), 7.62–7.72 (m, 4H), 4.38 (s, 2H), 3.40 (t, *J* = 7.9 Hz, 2H), 3.28 (t, *J* = 7.9 Hz, 2H), 3.12–3.22 (m, 8 H), 2.26–2.34 (m, 2H), 2.09–2.14 (m, 2H), 1.82–1.86 (m, 4H). ESI-MS *m/z*: 386.4 (M+H–4HCl)<sup>+</sup>. Anal. calcd for C<sub>22</sub>H<sub>39</sub>Cl<sub>4</sub>N<sub>5</sub>O·0.2 H<sub>2</sub>O: C, 49.39; H, 7.42; N, 13.09; found: C, 49.11; H, 7.60; N, 12.96.

#### 4.12. *N*-(Anthracen-9-yl)-2-(diethylamino)acetamide hydrochloride (6f)

Pale yellow solid, yield 66.8%, <sup>1</sup>H NMR (400 MHz, D<sub>2</sub>O) δ<sub>H</sub>: 8.60 (s, 1H), 8.10 (d, *J* = 7.8 Hz, 2H), 7.97 (d, *J* = 8.6 Hz, 2H), 7.52–7.61 (m, 4H), 4.60 (s, 2H), 3.40 (q, *J* = 7.4 Hz, 4H), 1.38 (t, *J* = 7.3 Hz, 6H). ESI-MS *m/z*: 307.2 (M+H–HCl)<sup>+</sup>. Anal. calcd for C<sub>20</sub>H<sub>23</sub>ClN<sub>2</sub>O·0.4 H<sub>2</sub>O: C, 68.62; H, 6.85; N, 8.00; found: C, 68.47; H, 6.92; N, 7.96.

#### 4.13. *N*-(anthracen-9-yl)-2-(cyclopropylamino)acetamide hydrochloride (6g)

Pale yellow solid, yield 67.2%, <sup>1</sup>H NMR (400 MHz, D<sub>2</sub>O) δ<sub>H</sub>: 8.67 (s, 1H), 8.16 (d, *J* = 8.2 Hz, 2H), 8.07 (d, *J* = 8.6 Hz, 2H), 7.57–7.65 (m, 4H), 4.55 (s, 2H), 2.89–2.95 (m, 1H), 0.99 (d, *J* = 5.6 Hz, 4H). ESI-MS *m/z*: 291.1 (M+H–HCl)<sup>+</sup>. Anal. calcd for C<sub>19</sub>H<sub>19</sub>ClN<sub>2</sub>O·0.1 H<sub>2</sub>O: C, 69.44; H, 5.89; N, 8.52; found: C, 69.39; H, 5.90; N, 8.43.

#### 4.14. *N*-(Anthracen-9-yl)-2-(3-hydroxypropylamino)acetamide hydrochloride (6h)

Pale yellow solid, yield 65.9%, <sup>1</sup>H NMR (400 MHz, D<sub>2</sub>O) δ<sub>H</sub>: 8.50 (s, 1H), 8.02 (d, *J* = 8.4 Hz, 2H), 7.94 (d, *J* = 8.6 Hz, 2H), 7.46–7.55 (m, 4H), 4.44 (s, 2H), 3.69 (t, *J* = 6.0 Hz, 2H), 3.28 (t, *J* = 7.7 Hz, 2H), 1.92–1.99 (m, 2H). ESI-MS *m/z*: 309.1 (M+H–HCl)<sup>+</sup>. Anal. calcd for C<sub>19</sub>H<sub>21</sub>ClN<sub>2</sub>O<sub>2</sub>·0.2 H<sub>2</sub>O: C, 65.49; H, 6.19; N, 8.04; found: C, 65.43; H, 6.02; N, 7.96.

#### 4.15. *N*-(Anthracen-9-yl)-2-(2-(dimethylamino)ethylamino)acetamide hydrochloride (6i)

Pale yellow solid, yield 64.8%, <sup>1</sup>H NMR (400 MHz, D<sub>2</sub>O) δ<sub>H</sub>: 8.59 (s, 1H), 8.09 (d, *J* = 8.2 Hz, 2H), 8.01 (d, *J* = 8.7 Hz, 2H), 7.51–7.61 (m, 4H), 4.59 (s, 2H), 3.70 (t, *J* = 7.9 Hz, 2H), 3.62 (t, *J* = 7.5 Hz, 2H), 2.96 (s, 6H). ESI-MS *m/z*: 322.2 (M+H–2.3HCl)<sup>+</sup>. Anal. calcd for C<sub>20</sub>H<sub>25</sub>Cl<sub>2</sub>N<sub>3</sub>O·0.3 HCl: C, 59.27; H, 6.29; N, 10.37; found: C, 59.25; H, 6.47; N, 10.16.

#### 4.16. 2-(3-Aminopropylamino)-N-(anthracen-9-yl)acetamide hydrochloride (6j)

Pale yellow solid, yield 69.2%,  $^1\text{H NMR}$  (400 MHz,  $\text{D}_2\text{O}$ )  $\delta_{\text{H}}$ : 8.59 (s, 1H), 8.08 (d,  $J = 30.2$  Hz, 4H), 7.57–7.63 (m, 4H), 4.57 (s, 2H), 3.37 (t,  $J = 7.7$  Hz, 2H), 3.15 (t,  $J = 7.7$  Hz, 2H), 2.16–2.24 (m, 2H). ESI-MS  $m/z$ : 308.2 (M+H–2HCl) $^+$ . Anal. calcd for  $\text{C}_{19}\text{H}_{23}\text{Cl}_2\text{N}_2\text{O}\cdot 0.6 \text{H}_2\text{O}$ : C, 58.35; H, 6.24; N, 10.74; found: C, 58.42; H, 6.09; N, 10.59.

#### 4.17. 2-(4-Aminobutylamino)-N-(anthracen-9-yl)acetamide hydrochloride (6k)

Pale yellow solid, yield 74.2%,  $^1\text{H NMR}$  (400 MHz,  $\text{D}_2\text{O}$ )  $\delta_{\text{H}}$ : 8.61 (s, 1H), 8.10 (d,  $J = 8.4$  Hz, 2H), 8.01 (d,  $J = 8.7$  Hz, 2H), 7.52–7.61 (m, 4H), 4.49 (s, 2H), 3.26 (t,  $J = 7.4$  Hz, 2H), 3.01 (t,  $J = 7.7$  Hz, 2H), 1.73–1.87 (m, 4H). ESI-MS  $m/z$ : 322.2 (M+H–2HCl) $^+$ . Anal. calcd for  $\text{C}_{20}\text{H}_{25}\text{Cl}_2\text{N}_3\text{O}\cdot 0.4 \text{H}_2\text{O}$ : C, 59.82; H, 6.48; N, 10.46; found: C, 59.90; H, 6.43; N, 10.40.

#### 4.18. 2-(6-Aminohexylamino)-N-(anthracen-9-yl)acetamide hydrochloride (6l)

White solid, yield 71.4%,  $^1\text{H NMR}$  (400 MHz,  $\text{D}_2\text{O}$ )  $\delta_{\text{H}}$ : 8.69 (s, 1H), 8.20 (d,  $J = 7.6$  Hz, 2H), 8.11 (d,  $J = 8.7$  Hz, 2H), 7.63–7.72 (m, 4H), 4.58 (s, 2H), 3.33 (t,  $J = 7.7$  Hz, 2H), 3.06 (t,  $J = 7.5$  Hz, 2H), 1.84–1.92 (m, 2H), 1.72–1.79 (m, 2H), 1.51–1.54 (m, 4H). ESI-MS  $m/z$ : 349.3 (M+H–2HCl) $^+$ . Anal. calcd for  $\text{C}_{22}\text{H}_{31}\text{Cl}_2\text{N}_3\text{O}_2$ : C, 60.00; H, 7.09; N, 9.54; found: C, 59.93; H, 7.06; N, 9.44.

#### 4.19. 2-(3-(3-Aminopropylamino)propylamino)-N-(anthracen-9-yl)acetamide hydrochloride (6m)

Yellow solid, yield 69.6%,  $^1\text{H NMR}$  (400 MHz,  $\text{D}_2\text{O}$ )  $\delta_{\text{H}}$ : 8.72 (s, 1H), 8.23 (d,  $J = 8.4$  Hz, 2H), 8.14 (d,  $J = 8.7$  Hz, 2H), 7.65–7.74 (m, 4H), 4.66 (s, 2H), 3.47 (t,  $J = 7.5$  Hz, 2H), 3.25–3.35 (m, 4H), 3.18 (t,  $J = 7.8$  Hz, 2H), 2.29–2.37 (m, 2H), 2.14–2.22 (m, 2H). ESI-MS  $m/z$ : 365.3 (M+H–3HCl) $^+$ . Anal. calcd for  $\text{C}_{22}\text{H}_{33}\text{Cl}_3\text{N}_4\text{O}_2\cdot 0.1 \text{H}_2\text{O}$ : C, 53.52; H, 6.78; N, 11.25; found: C, 53.78; H, 6.81; N, 10.95.

#### 4.20. 2-(4-(3-Aminopropylamino)butylamino)-N-(anthracen-9-yl)acetamide hydrochloride (6n)

Light white solid, yield 64.6%,  $^1\text{H NMR}$  (400 MHz,  $\text{D}_2\text{O}$ )  $\delta_{\text{H}}$ : 8.42 (s, 1H), 7.96 (d,  $J = 8.4$  Hz, 2H), 7.92 (d,  $J = 8.8$  Hz, 2H), 7.41–7.52 (m, 4H), 4.44 (s, 2H), 3.20 (t,  $J = 7.5$  Hz, 2H), 2.96–3.06 (m, 6H), 1.94–2.02 (m, 2H), 1.71–1.81 (m, 4H). ESI-MS  $m/z$ : 379.3 (M+H–3HCl) $^+$ . Anal. calcd for  $\text{C}_{23}\text{H}_{33}\text{Cl}_3\text{N}_4\text{O}\cdot 0.7 \text{H}_2\text{O}$ : C, 55.19; H, 6.93; N, 11.19; found: C, 55.36; H, 7.06; N, 10.90.

#### 4.21. 2-(3-(4-(3-Aminopropylamino)butylamino)propylamino)-N-(anthracen-9-yl)acetamide hydrochloride (6o)

Pale yellow solid, yield 62.9%,  $^1\text{H NMR}$  (400 MHz,  $\text{D}_2\text{O}$ )  $\delta_{\text{H}}$ : 8.56 (s, 1H), 8.06 (d,  $J = 8.5$  Hz, 2H), 7.99 (d,  $J = 8.8$  Hz, 2H), 7.49–7.58 (m, 4H), 4.52 (s, 2H), 3.31 (t,  $J = 7.9$  Hz, 2H), 3.15 (t,  $J = 8.0$  Hz, 2H), 3.00–3.09 (m, 8 H), 2.13–2.21 (m, 2H), 1.97–2.05 (m, 2H), 1.69–1.73 (m, 4H). ESI-MS  $m/z$ : 436.4 (M+H–4HCl) $^+$ . Anal. calcd for  $\text{C}_{26}\text{H}_{43}\text{Cl}_4\text{N}_5\text{O}_2\cdot 0.4 \text{H}_2\text{O}$ : C, 51.47; H, 7.28; N, 11.54; found: C, 51.48; H, 7.50; N, 11.30.

#### 4.22. General procedures for the preparation of intermediates 5p–5s

A mixture of polyamine (**4a**, **4f**, **4i** or **4j**) (3 mmol),  $\text{K}_2\text{CO}_3$  (0.83 g, 6.0 mmol), KI (catalytic amount) in  $\text{CH}_3\text{CN}$  (40 mL) was

stirred at room temperature for 30 min, then intermediate **3a** (0.9 g, 3 mmol) was added and stirred at room temperature for 24 h (monitored by TLC). The solvent was removed in vacuum, the residue was diluted with  $\text{CH}_2\text{Cl}_2$  (35 mL) and then washed with 10%  $\text{NaCO}_3$  (30 mL  $\times$  3). The organic layer was dried over  $\text{NaSO}_4$ , filtered, concentrated in vacuo, and purified by flash column chromatography with chloroform/methanol elution to give **5p–5s**.

#### 4.23. General procedures for the preparation of the target compounds 6p–6s

The respective *N*-Boc protected intermediates **5p–5s** were dissolved in EtOH (10 mL) and stirred at 0 °C for 10 min. Then 4 M HCl was added dropwise at 0 °C. The reaction mixture was stirred at room temperature overnight. The solution typically gave a pale yellow solid as a precipitate. The solid was concentrated and washed several times with absolute ethanol and ether, and dried under vacuum to give the pure target compounds **6a–6s**.

#### 4.24. N-(9,10-dioxo-9,10-dihydroanthracen-1-yl)-2-(3-hydroxypropylamino)acetamide hydrochloride (6p)

Orange solid, yield 68.8%,  $^1\text{H NMR}$  (400 MHz,  $\text{D}_2\text{O}$ )  $\delta_{\text{H}}$ : 8.36 (d,  $J = 9.4$  Hz, 1H), 7.67–7.76 (m, 4H), 7.52–7.55 (m, 2H), 4.29 (s, 2H), 3.91 (t,  $J = 5.7$  Hz, 2H), 3.48 (t,  $J = 7.4$  Hz, 2H), 2.13–2.20 (m, 2H). ESI-MS  $m/z$ : 339.2 (M+H–HCl) $^+$ . Anal. calcd for  $\text{C}_{19}\text{H}_{19}\text{ClN}_2\text{O}_4\cdot 0.3 \text{H}_2\text{O}$ : C, 60.02; H, 5.20; N, 7.37; found: C, 59.93; H, 7.31; N, 7.31.

#### 4.25. 2-(4-Aminobutylamino)-N-(9,10-dioxo-9,10-dihydroanthracen-1-yl)acetamide hydrochloride (6q)

Bright yellow solid, yield 76.2%,  $^1\text{H NMR}$  (400 MHz,  $\text{D}_2\text{O}$ )  $\delta_{\text{H}}$ : 8.46 (d,  $J = 6.8$  Hz, 1H), 7.84–7.88 (m, 2H), 7.62–7.76 (m, 4H), 4.33 (s, 2H), 3.38 (t,  $J = 7.3$  Hz, 2H), 3.18 (t,  $J = 7.7$  Hz, 2H), 1.88–2.04 (m, 4H). ESI-MS  $m/z$ : 352.2 (M+H–2HCl) $^+$ . Anal. calcd for  $\text{C}_{20}\text{H}_{23}\text{Cl}_2\text{N}_3\text{O}_3\cdot 0.2 \text{H}_2\text{O}$ : C, 56.13; H, 5.51; N, 9.82; found: C, 56.06; H, 5.18; N, 9.63.

#### 4.26. 2-(4-(3-Aminopropylamino)butylamino)-N-(9,10-dioxo-9,10-dihydroanthracen-1-yl)acetamide hydrochloride (6r)

Bright yellow solid, yield 80.8%,  $^1\text{H NMR}$  (400 MHz,  $\text{D}_2\text{O}$ )  $\delta_{\text{H}}$ : 8.48 (d,  $J = 8.3$  Hz, 1H), 7.86–7.90 (m, 2H), 7.73–7.78 (m, 4H), 7.66 (t,  $J = 8.1$  Hz, 1H), 4.34 (s, 2H), 3.38 (t,  $J = 7.0$  Hz, 2H), 3.24–3.28 (m, 4H), 3.19 (t,  $J = 7.8$  Hz, 2H), 2.14–2.22 (m, 2H), 1.91–2.04 (m, 4H). ESI-MS  $m/z$ : 309.3 (M+H–3HCl) $^+$ . Anal. calcd for  $\text{C}_{23}\text{H}_{31}\text{Cl}_3\text{N}_4\text{O}_3\cdot 0.1 \text{H}_2\text{O}$ : C, 53.16; H, 6.05; N, 10.78; found: C, 53.07; H, 5.74; N, 10.68.

#### 4.27. 2-(3-(4-(3-Aminopropylamino)butylamino)propylamino)-N-(9,10-dioxo-9,10-dihydroanthracen-1-yl)acetamide hydrochloride (6s)

Bright yellow solid, yield 64.7%,  $^1\text{H NMR}$  (400 MHz,  $\text{D}_2\text{O}$ )  $\delta_{\text{H}}$ : 8.52 (d,  $J = 8.4$  Hz, 1H), 7.95–8.00 (m, 2H), 7.69–7.83 (m, 3H), 4.36 (s, 2H), 3.40 (t,  $J = 7.9$  Hz, 2H), 3.28 (t,  $J = 7.9$  Hz, 2H), 3.12–3.22 (m, 8 H), 2.26–2.34 (m, 2H), 2.09–2.14 (m, 2H), 1.82–1.86 (m, 4H). ESI-MS  $m/z$ : 465.5 (M+H–4HCl) $^+$ . Anal. calcd for  $\text{C}_{26}\text{H}_{39}\text{Cl}_4\text{N}_5\text{O}_3\cdot 0.1 \text{H}_2\text{O}$ : C, 50.92; H, 6.44; N, 11.42; found: C, 51.04; H, 6.15; N, 11.11.

### 5. Biological activity

#### 5.1. In vitro inhibition studies on AChE and BChE

Acetylcholinesterase (AChE, E.C. 3.1.1.7, from *electric eel*), butyrylcholinesterase (BChE, E.C. 3.1.1.8, from *equine serum*), 5,5'-dithi-

obis-(2-nitrobenzoic acid) (Ellman's reagent, DTNB), acetylthiocholine chloride (ATC), butylthiocholine chloride (BTC), and tacrine were purchased from Sigma Aldrich. Tacrine and synthesized derivatives were dissolved in H<sub>2</sub>O and then diluted in 0.1 M KH<sub>2</sub>PO<sub>4</sub>/K<sub>2</sub>HPO<sub>4</sub> buffer (pH 8.0) to provide a final concentration range.

All the assays were under 0.1 M KH<sub>2</sub>PO<sub>4</sub>/K<sub>2</sub>HPO<sub>4</sub> buffer, pH 8.0, using a Shimadzu UV-2450 Spectrophotometer. Enzyme solutions were prepared to give 2.0 units/mL in 2 mL aliquots. The assay medium contained phosphate buffer, pH 8.0 (1 mL), 50  $\mu$ L of 0.01 M DTNB, 10  $\mu$ L of enzyme, and 50  $\mu$ L of 0.01 M substrate (ATC). The substrate was added to the assay medium containing enzyme, buffer, and DTNB with inhibitor after 15 min of incubation time. The activity was determined by measuring the increase in absorbance at 412 nm at 1 min intervals at 37 °C. Calculations were performed according to the method of the equation in Ellman et al. In vitro BChE assay use the similar method described above. Each concentration was assayed in triplicate.

## 5.2. Kinetic characterization of AChE inhibition

Six different concentrations of substrate were mixed in the 1 mL 0.1 M KH<sub>2</sub>PO<sub>4</sub>/K<sub>2</sub>HPO<sub>4</sub> buffer (pH 8.0), containing 50  $\mu$ L of DTNB, 10  $\mu$ L AChE, and 50  $\mu$ L substrate. Test compound was added into the assay solution and pre-incubated with the enzyme at 37 °C for 15 min, followed by the addition of substrate. Kinetic characterization of the hydrolysis of ATC catalyzed by AChE was done spectrometrically at 412 nm. A parallel control with no inhibitor in the mixture, allowed adjusting activities to be measured at various times. BChE assay use the similar method described above.

## 6. Molecular modeling

The crystal structure of the torpedo AChE complexed with tacrine (code ID: 1ACJ) was obtained in the Protein Data Bank after eliminating the inhibitor and water molecules. The 3D Structure of **6I** was built and performed geometry optimization by molecular mechanics. Further preparation of substrates included addition of Gasteiger charges, removal of hydrogen atoms and addition of their atomic charges to skeleton atoms, and finally, assignment of proper atomic types. Autotors was then used to define the rotatable bonds in the ligand.

Docking studies were carried out using the AUTODOCK 4.0 program. Using ADT, Polar hydrogen atoms were added to amino acid residues and Gasteiger charges were assigned to all atoms of the enzyme. The resulting enzyme structure was used as an input for the AUTOGRID program. AUTOGRID performed a precalculated atomic affinity grid maps for each atom type in the ligand plus an electrostatics map and a separate desolvation map present in the substrate molecule. All maps were calculated with 0.375 Å spacing between grid points. The centre of the grid box was placed at the bottom of the active site gorge (AChE [2.781 64.383 67.971]). The dimensions of the active site box were set at 50  $\times$  46  $\times$  46 Å.

Flexible ligand docking was performed for the compounds. Docking calculations were carried out using the Lamarckian genetic algorithm (LGA) and all parameters were the same for each docking. To ensure the reliability of the results, the docking procedures were repeated 10 independent times for the compound and the obtained orientations were analyzed.

## 7. MTT assay of HepG2 cell viability

Cells were cultured at 37 °C under a 5% CO<sub>2</sub> atmosphere. The antiproliferative ability of compounds was evaluated in HepG2

cells by the conversion of MTT to a purple formazan precipitate as previously described.<sup>24</sup> Cells were seeded into 96-well plates at  $5 \times 10^3$  cells/well. After 12 h, 0.1, 1.0, 10, 30, 100  $\mu$ M of compounds were subsequently added and incubated for 48 h. The cell viability was determined by using MTT colorimetry, measuring the absorption at 590 nm. Controls were taken as having 100% viability. Each concentration was tested in triplicate, and IC<sub>50</sub> values were calculated graphically from log concentration–inhibition curve (Origin 7.5 software).

## Acknowledgments

We thank the Natural Science Foundation of China (Nos. 21172053, 21302041), the Postdoctoral Science Foundation of China (No. 2012M521391), and the Postdoctoral Science Foundation of Henan Province (No. 2011015) for financial support of this study.

## Supplementary data

Supplementary data associated with this article can be found, in the online version, at <http://dx.doi.org/10.1016/j.bmc.2014.03.045>.

## References and notes

- Kung, H. F.; Lee, C. W.; Zhuang, Z. P.; Kung, M. P.; Hou, C.; Plössl, K. J. *Am. Chem. Soc.* **2001**, *123*, 12740.
- Förstl, H.; Kurz, A. *Eur. Arch. Psychiatry Clin. Neurosci.* **1999**, *249*, 288.
- Cummings, J. L.; Doody, R.; Clark, C. *Neurology* **2007**, *69*, 1622.
- Cavalli, A.; Bolognesi, M. L.; Minarini, A.; Rosini, M.; Tumiatti, V.; Recanatini, M.; Melchiorre, C. *J. Med. Chem.* **2008**, *51*, 347.
- Meng, F. C.; Mao, F.; Shan, W. J.; Qin, F.; Huang, L.; Li, X. S. *Bioorg. Med. Chem. Lett.* **2012**, *22*, 4462.
- Greig, N. H.; Utsuki, T.; Ingram, D. K.; Wang, Y.; Pepeu, G.; Scali, C.; Yu, Q. S.; Mamczarz, J.; Holloway, H. W.; Giordano, T.; Chen, D.; Furukawa, K.; Sambamurti, K.; Brossi, A.; Lahiri, D. K. *Proc. Natl. Acad. Sci. U.S.A.* **2005**, *102*, 17213.
- Woo, Y. J.; Lee, B. H.; Yeun, G. H.; Kim, H. J.; Won, M. H.; Kim, S. H.; Lee, B. L.; Park, J. H. *Bull. Korean Chem. Soc.* **2011**, *32*, 2593.
- Tumiatti, V.; Milelli, A.; Minarini, A.; Rosini, M.; Bolognesi, M. L.; Micco, M.; Andrisano, V.; Bartolini, M.; Mancini, F.; Recanatini, M.; Cavalli, A.; Melchiorre, C. *J. Med. Chem.* **2008**, *51*, 7308.
- Bolognesi, M. L.; Banzi, R.; Bartolini, M.; Cavalli, A.; Tarozzi, A.; Andrisano, V.; Minarini, A.; Rosini, M.; Tumiatti, V.; Bergamini, C.; Fato, R.; Lenaz, G.; Hrelia, P.; Cattaneo, A.; Recanatini, M.; Melchiorre, C. *J. Med. Chem.* **2007**, *50*, 4882.
- Simoni, E.; Bergamini, C.; Fato, R.; Tarozzi, A.; Bains, S.; Motterlini, R.; Cavalli, A.; Bolognesi, M. L.; Minarini, A.; Hrelia, P.; Lenaz, G.; Rosini, M.; Melchiorre, C. *J. Med. Chem.* **2010**, *53*, 7264.
- Cen, J.; Liu, L.; He, L.; Liu, M.; Wang, C. J.; Ji, B. S. *Int. J. Dev. Neurosci.* **2012**, *30*, 584.
- Elsinghorst, P. W.; Hartig, W.; Gundisch, D.; Mohr, K.; Trankle, C.; Gutschow, M. *Curr. Top. Med. Chem.* **2011**, *11*, 2731.
- Tian, Z. Y.; Xie, S. Q.; Mei, Z. H.; Zhao, J.; Gao, W. Y.; Wang, C. J. *Org. Biomol. Chem.* **2009**, *7*, 4651.
- Xie, S. Q.; Wang, J. H.; Ma, H. X.; Cheng, P. F.; Zhao, J.; Wang, C. J. *Toxicology* **2009**, *263*, 127.
- Wang, J. H.; Chen, Z. Y.; Xie, S. Q.; Zhao, J.; Wang, C. J. *Bioorg. Med. Chem. Lett.* **2010**, *20*, 6421.
- Wang, Y. X.; Zhang, X. B.; Zhao, J.; Xie, S. Q.; Wang, C. J. *J. Med. Chem.* **2012**, *55*, 3502.
- Luo, W.; Huang, K.; Zhang, Z.; Hong, C.; Wang, Y. Q. *Acta Pharmacol. Sin.* **2013**, *48*, 269.
- Sheu, S. Y.; Chiang, H. C. *Anticancer Res.* **1997**, *17*, 3293.
- Shi, D. H.; Huang, W.; Li, C.; Wang, L. T.; Wang, S. F. *Bioorg. Med. Chem.* **2013**, *21*, 1064.
- Ellman, G. L.; Courtney, K. D., Jr.; Andres, B.; Featherstone, R. M. *Biochem. Pharmacol.* **1961**, *7*, 88.
- Tang, H.; Ning, F. X.; Wei, Y. B.; Huang, S. L.; Huang, Z. S.; Chan, A. S.; Gu, L. Q. *Bioorg. Med. Chem. Lett.* **2007**, *17*, 3765.
- Morris, G. M.; Goodsell, D. S.; Halliday, R. S.; Huey, R.; Hart, W. E.; Belew, R. K.; Olson, A. J. *J. Comput. Chem.* **1998**, *19*, 1639.
- DeLano, W.L. The PyMOL Molecular Graphics System. DeLano Scientific. San Carlos, CA, 2002
- Mosmann, T. *J. Immunol. Methods* **1983**, *65*, 55.